JTTEE5 13:57-65
DOI: 10.1361/10599630418121
1059-9630/$19.00 © ASM International

Superior Thermal Barrier Coatings Using Solution Precursor Plasma Spray

E.H. Jordan, L. Xie, X. Ma, M. Gell, N.P. Padture, B. Cetegen, A. Ozturk, J. Roth, T.D. Xiao, and P.E.C. Bryant

(Submitted 21 August 2003; in revised form 15 October 2003)

A novel process, solution precursor plasma spray (SPPS), is presented for depositing thermal barrier coatings (TBCs), in which aqueous chemical precursors are injected into a standard direct current plasma spray system. The resulting coatings microstructure has three unique features: (1) ultra fine splats (1 μm), (2) nanometer and micron-sized interconnected porosity, and (3) closely spaced, through-thickness cracks. Coatings over 3 mm thick can be readily deposited using the SPPS process. Coating durability is excellent, with SPPS coatings showing, in furnace cycling tests, 2.5 times the spallation life of air plasma coatings (APS) and 1.5 times the life of electron beam physical vapor deposited (EB-PVD) coatings. The conductivity of SPPS coatings is lower than EB-PVD coatings and higher than the best APS coatings. Manufacturing cost is expected to be similar to APS coatings and much lower than EB-PVD coatings. The SPPS deposition process includes droplet break-up and material arriving at the deposition surface in various physical states ranging from aqueous solution, gel phase, to fully-molten ceramic. The relation between the arrival state of the material and the microstructure is described.

Keywords solution precursor plasma spray, thermal barrier coatings

1. Introduction

Gas turbine hot section components are subjected to hot gases with temperatures exceeding the melting temperature of the alloys from which they are made. As a result component designs include critically important features to reduce metal temperatures, which include internal and film cooling and the application of ceramic insulating thermal barrier coatings (TBCs).

Current TBCs are ceramic insulating layers, which are deposited on the metallic component to reduce metal temperatures by as much as 150 °C. The extensive literature on the properties and failure behavior of such coatings can be found in several recent reviews.[1,2] Current production coatings are made predominantly of 7 wt.% Y_2O_3 stabilized ZrO_2. These coatings are made either by air plasma spray (APS) or by electron beam physical vapor deposition (EB-PVD). In general EB-PVD TBCs have superior durability but have higher thermal conductivity and higher cost compared with APS TBCs.

In the present paper, a third method of making TBCs is presented where the motivation for developing another processing method is to provide improved properties compared with current practice. This novel method-solution precursor plasma spray (SPPS) is based on the injection of liquid chemical precursors into a plasma jet and forming a ceramic by pyrolosis in the plasma jet. Synthesis of powder materials by similar processes has been carried out for a variety of materials[3] and coatings have been made by related processes for other material systems.[4-6] In our earlier publications, various aspects of the production of TBCs by the SPPS process have been presented.[7-11] In the present paper, we seek to provide an overview of the work to date, with emphasis on the performance of the coatings and the related microstructures and deposition mechanisms.

E.H. Jordan, L. Xie, M. Gell, N.P. Padture, B. Cetegen, and **A. Ozturk,** University of Connecticut, Storrs, CT 06269-3137; and **X. Ma, J. Roth, T.D. Xiao,** and **P.E. C. Bryant,** Inframat Inc., Farmington, CT 06032. Contact e-mail: jordan@engr.uconn.edu.

2. Description of the Process

Figure 1 shows the basic configuration for the SPPS process. In this process an aqueous solution of the constituent metal salts (Zr and Y) is atomized and injected into a direct current (dc) arc plasma jet. The ceramic is formed by pyrolysis in the plasma jet prior to reaching the target material or in some cases after reaching the surface. This spray method is identical to APS deposition with the substitution of a solution atomizer for the solid powder feeder. The atomization characteristics can be varied, but it involves initial droplet sizes between 20 and 50 μm at various velocities up to 100 m/s.[10] Plasma torch operating power and gas flow rates are in the same range as used for depositing APS coatings.

3. Experimental Methods

All SPPS coatings shown were made using a Metco 9MB spray system with a 3 MB gas-handling panel. The primary gas used was argon and the secondary gas was hydrogen. A custom made fluid delivery system that consists of a precursor storage tank with a regulated nitrogen overpressure that drives fluid through a hose to a gas atomizing nozzle mounted at 90° from the gun axis. Nitrogen was used as the atomizing gas.

Coating cross sections were made by sectioning the sample on a diamond saw and mounting the samples in epoxy. Following mounting, the samples were polished using standard meth-

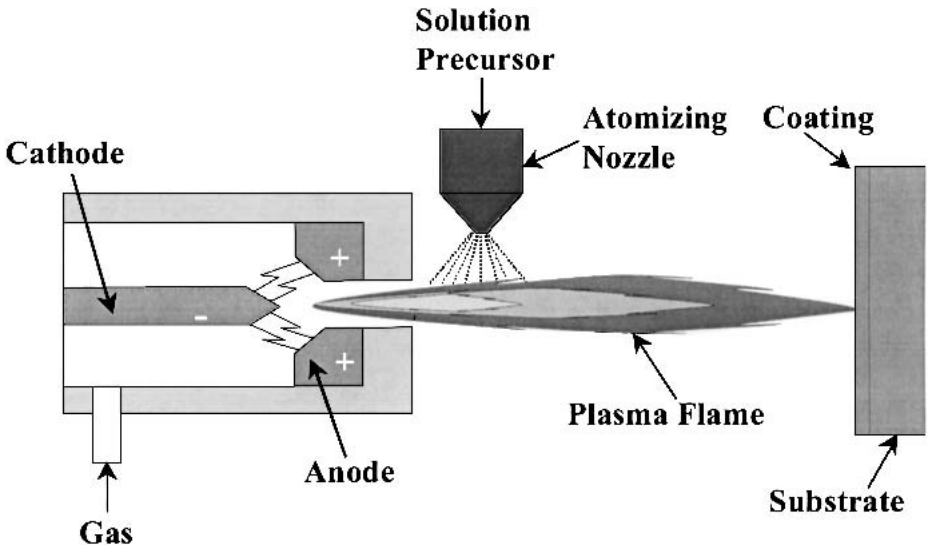

Fig. 1 Schematic illustration of the SPPS process

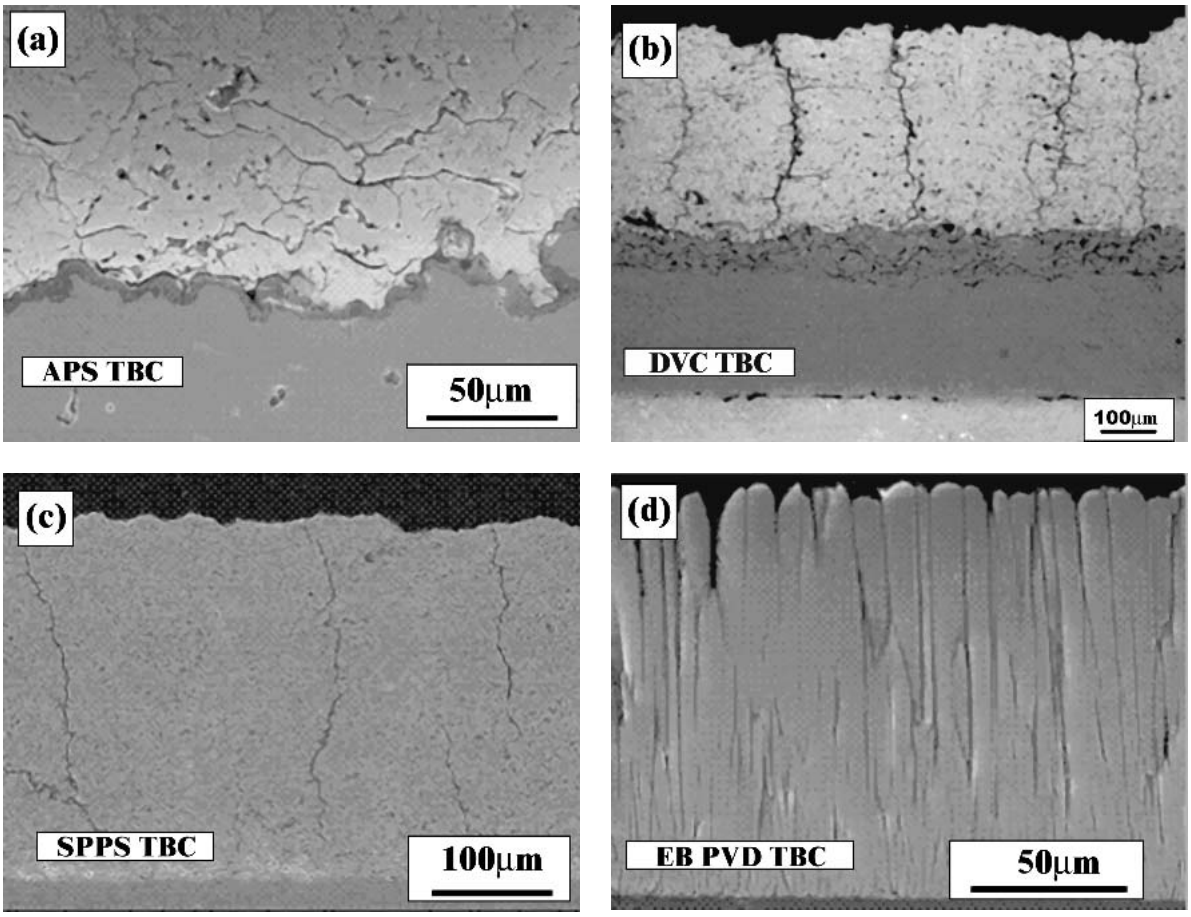

Fig. 2 Comparison of SPPS microstructure with DVC TBC, APS TBC, and EB-PVD TBC

ods, ending with a 0.05 μm alumina paste. Samples were examined in a Phillips (ESEM2020) environmental scanning electron microscope or with a JEOL (JSM6355F) field emission scanning electron microscope. Some coating cross sections were prepared by notching the sample with a diamond saw and fracturing them in bending to reveal ultrafine splats. This is necessary be-

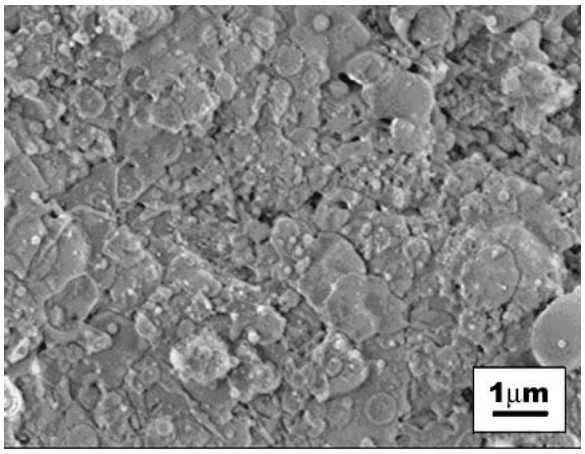

(a)

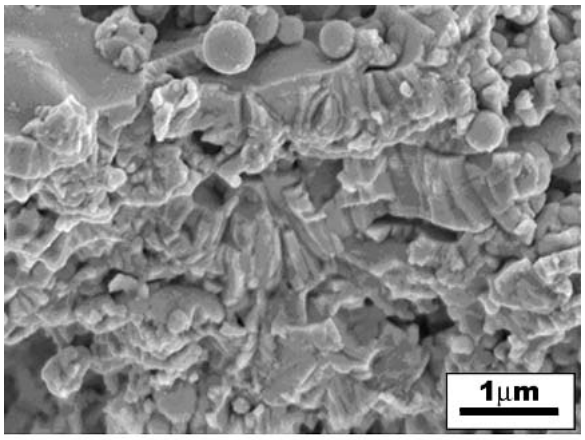

(b)

Fig. 3 **(a)** Ultrafine splats: top view, **(b)** cross section view

cause simple fracture leads to failure at the vertical cracks revealing an atypical microstructure. Cyclic furnace durability tests with a 1 h cycle time and a maximum temperature of 1121 °C were run in an elevator furnace. The SPPS coasting used in the cyclic furnace tests had a porosity of 18% as determined by the Archimedes method and had an average thickness of 300 μm. The cycle consisted of a 10 min heat up, a 40 min hold at the maximum temperature, and 5 min of forced air-cooling.

4. Major Microstructural Features

The microstructure of a typical SPPS coating optimized for use as a TBC is shown in Fig. 2 along with microstructures of EB-PVD, dense vertically cracked (DVC) and APS TBCs for comparison. There are four important microstructural features

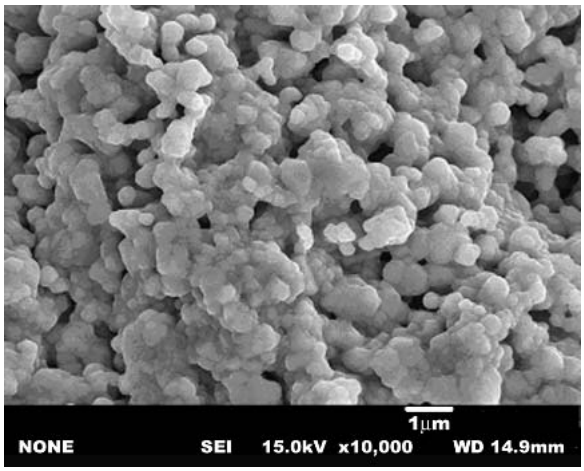

Fig. 4 Nano and micrometer porosity

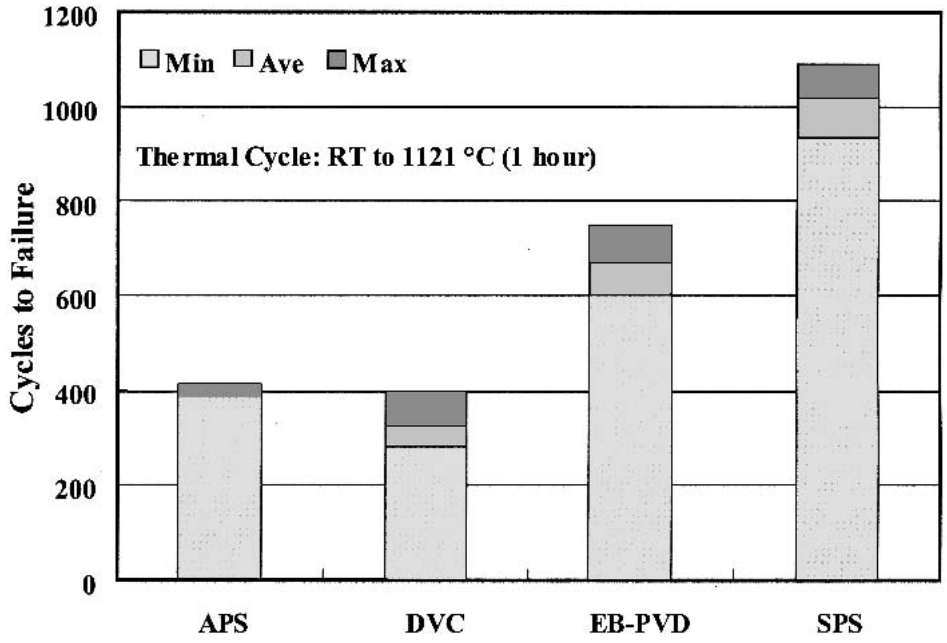

Fig. 5 Comparison of the cyclic life of SPPS coatings and other commercial coating tested with a maximum cycle temperature of 1121 °C

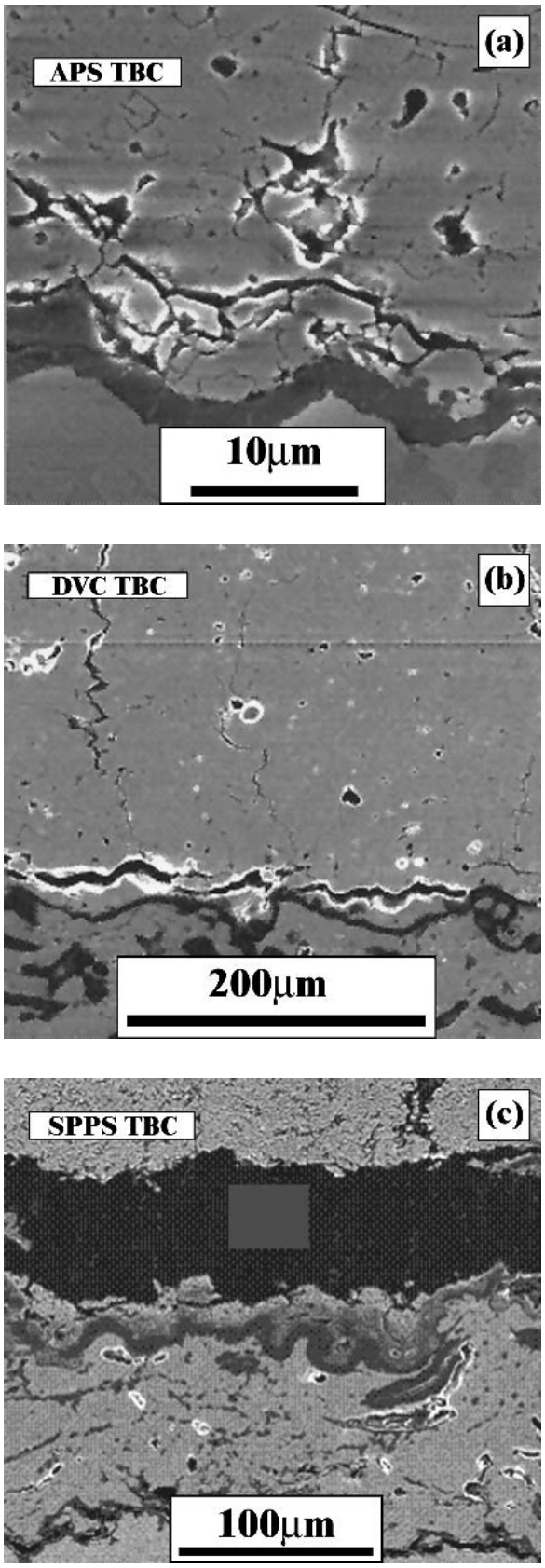

Fig. 6 Cross sections of SPPS, APS, and DVC coatings showing similar failure paths

of note in SPPS coatings: (1) the deposited ceramic is t′ tetragonal phase[8]; (2) there are vertical through thickness cracks (Fig. 2); (3) an ultrafine splat morphology is present (Fig. 3); and (4) micron and nanometer-sized interconnected porosity is present (Fig. 4).[8] This microstructure is different from EB-PVD microstructures where the coating has columnar grains with inter-columnar porosity and from APS coatings, which has a course splat microstructure with prominent transverse splat boundaries (Fig. 2). This APS coating had porosity approximately 20%. The SPPS microstructure differs from that of DVCs, which require a higher ceramic density (>88%) to produce through-thickness cracks and contain normal-sized splats.

5. TBC Performance

The three most important characteristics for TBCs are (1) excellent cyclic durability, (2) low thermal conductivity, and (3) low cost. In assessing these properties, 25 mm diameter samples on bond-coated superalloy substrates were used with the composition as shown in Table 1.

Cyclic furnace tests were performed using 1 h cycles with a maximum cycle temperature of 1121 °C. The same furnace and temperature cycle were used in our previous research programs providing a comparison data base, which includes approximately 10 variants (APS and EB-PVD) of bill of material coat-

Table 1 Chemical Composition of Alloys and Coatings Used

Material Layer	Composition in wt.%
SPPS TBC top coat	$7Y_2O^3$, balance ZrO_2
APS Bond coat	Co:33.5, Ni:32, Cr:22, Al:12, Y:0.5
Superalloy (H250)	Ni:57, Cr:22, W:14, Mn:0.5, Mo:2, Co:<5, Fe:<3

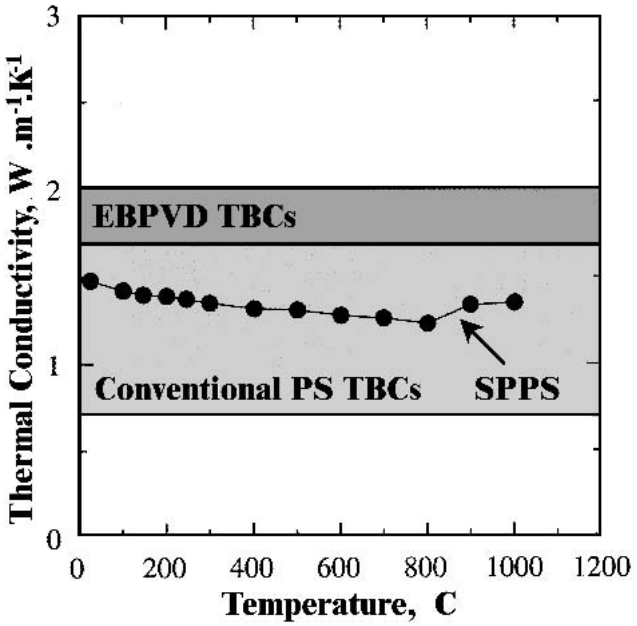

Fig. 7 Thermal conductivity as a function of temperature[7]

ing systems provided by engine and coating manufacturers. The life of the SPPS coated samples is shown in Fig. 5 along with spallation lives of a typical EB-PVD, DVC, and APS sample tested in the same rig. The SPPS mean life is the longest we have ever obtained in this test and is 2.5 times that of the APS TBCs, using the same substrate and bond coat, and 1.5 of the EB-PVD TBCs. X-ray diffraction confirms that the coating phase composition, which consisted of non-transformable T′ phase, was unaffected by thermal cycling. Figure 6 shows the failure mode for the SPPS coating compared with the APS and DVC coating. In all three cases, crack initiation and propagation are predominantly in the ceramic just above the TGO to ceramic interface. Thus, the SPPS coatings are still susceptible to similar failure mechanisms as other plasma sprayed coatings, but such processes take longer for SPPS coatings.

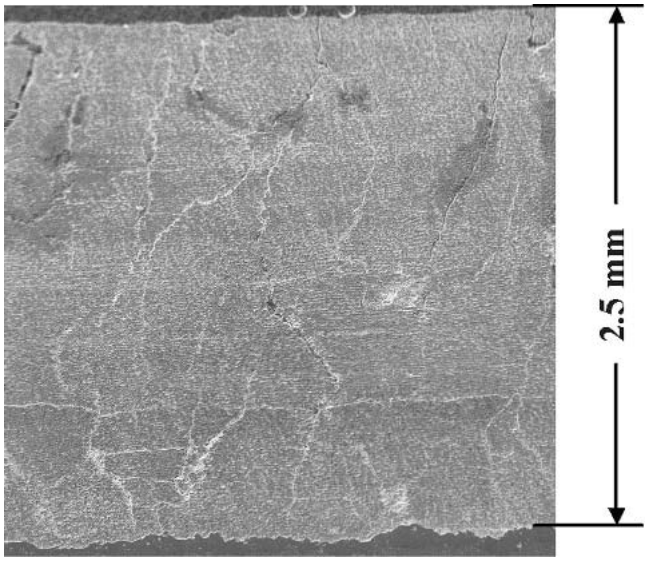

Fig. 8 Thick SPPS deposit cross section

Thermal conductivity determines the level of thermal protection for a given coating thickness. Figure 7 shows the thermal conductivity as a function of temperature[7] measured using the laser flash method for a nonoptimized SPPS coating. The conductivities typical of EB-PVD coatings and APS coatings are shown in Fig. 7 for comparison. The SPPS coating has lower conductivity than EB-PVD coatings but in the upper range found in APS coatings. There is considerable potential for lowering the thermal conductivity of SPPS coatings, which is being pursued presently.

The cost of making coatings is important. In the case of APS and EB-PVD TBCs, cost is well established, as they are production industrial processes. The cost of making SPPS coatings can be estimated based only on current practice and deposition rates. A cost analysis was performed, taking into consideration the utilization cost of the faculties, material costs, operator costs, and deposition rate/efficiencies. From this analysis, the SPPS coatings are expected to be much less costly than EB-PVD coatings and similar to the cost of APS coatings.

Finally, in some applications, such as combustors and blade outer air seals, the production of thick coatings is desirable. Due to low deposition rate, the production of very thick EB-PVD coatings is not practical. With careful attention to residual stress build-up, thick APS coatings can be produced. In the case of SPPS coatings, thick coatings can be made without any special processing other than coating for a longer time. A 2.5 mm thick coating is shown in Fig. 8. Interestingly the vertical crack spacing scales with the coating thickness such that the aspect ratio of the regions between the cracks remains roughly constant with a coating thickness to crack spacing, typically around 2.

Direct proof of the relationship between the SPPS microstructure and performance is still being developed. Much of the difference between SPPS and APS coatings appears to be related to the vertical cracks and smaller splats in SPPS coatings and

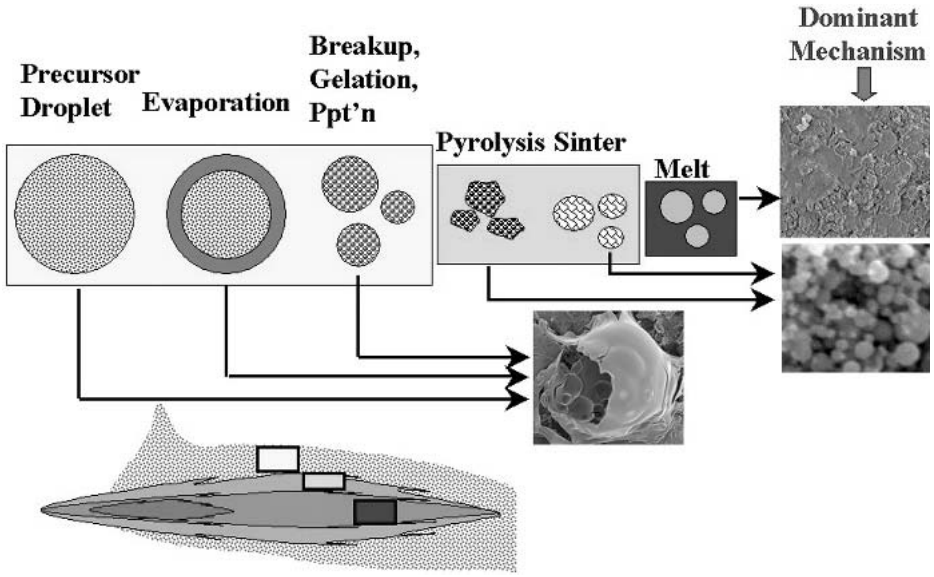

Fig. 9 Schematic illustration showing multiple paths for materials being deposited by the SPPS process

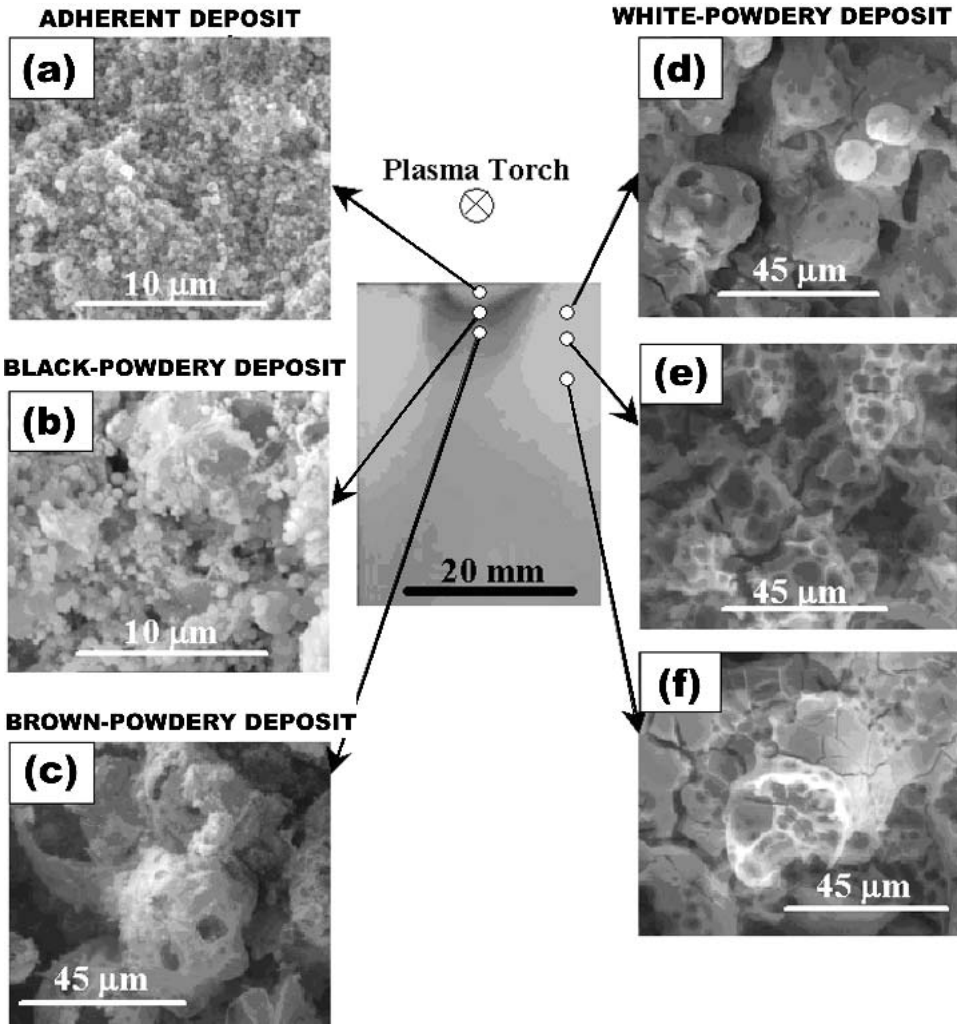

Fig. 10 Coating microstructure as a function of distance from plasma jet centerline

much smaller horizontal cracks. It is known that cracks lower thermal conductivity normal to the crack plane in proportion to the cube of the crack radius[12] making the larger cracks in APS coatings more effective at lowering thermal conductivity for a given crack density than the smaller cracks in SPPS coatings. This possibly explains the somewhat better thermal performance of APS coatings. On the other hand, it is known from fracture mechanics that strength generally goes down with the square root of the crack length, suggesting one possible reason for the superior mechanical performance of SPPS coating compared with APS coatings. A very important question currently under investigation is why SPPS coatings form vertical cracks. The precise mechanisms is not yet understood; however, the as-deposited coating always contains a significant amount of material not fully pyrolized, which will shrink dramatically when pyrolized.[8]

In summary, SPPS coatings have superior durability, lower cost, lower thermal conductivity, and greater practical thickness limits than EB-PVD. Compared with APS coatings, SPPS coatings have superior durability, with comparable cost and thermal conductivity.

6. Deposition Mechanisms

Understanding the deposition mechanisms in this process is desirable from a fundamental point of view and from a practical viewpoint because such understanding provides a basis for anticipating the effects of processing on microstructure and properties. The details of the experiments to elucidate the deposition mechanisms have been presented elsewhere.[9,13] Here we summarize the findings with only a conceptual description as to how the mechanisms were determined. Fundamentally, the process begins with the aqueous solution, which travels though the plasma jet and is deposited on the part surface. Figure 9 is a schematic illustration of the stages of evolution that the precursor goes though as it travels in the plasma jet to the sample surface. As noted in the Fig. 9, precursor in various stages of heating reaches the surface and contributes different features to the microstructure.

Initially, the precursor is atomized and injected perpendicular to the jet axis with a droplet size, which ranges from 20 to 45 μm,[8,10] and the injection location can be varied resulting in dif-

ferent degrees of heating, which leads to changes in the microstructure as will be discussed later. As would be expected, the plasma jet is hottest at its center, and as a result precursor that travels in the outer part of the jet arrives cooler than precursor traveling on the centerline. Figure 10 shows the deposition pattern from a stationary gun deposition experiments,[9] where a variation in the appearance of the deposits is seen to occur as a function of radial distance form the gun axis. Along the centerline, a dense deposit (Fig. 10a) is produced, which in cross section is seen (Fig. 2) to consist primarily of ultra fine splats. These features are similar to those present in conventional APS coatings but are much smaller in size with typical splat diameters of 1-2 μ compared with 50-100 μ in APS coatings. In addition, a number of crystalline spheres are incorporated into the microstructure (Fig. 3). Further from the centerline, two other types of deposits (Fig. 10) are found, hollow spheres (Fig. 10b) and further from the centerline, regions that turn out to be "mud flat" cracked non-crystalline gel phase precursor deposits (Fig. 10f) are found. Thermo-gravimetric analysis (TGA) shows[11] that the "mudflat"-cracked regions contain water. Changing the processing parameters can vary the relative proportion of the three major types of deposits. Under very hot spray conditions, 95% fully dense coatings can be produced. In the case of optimized TBCs, the deposited volume fractions of voids, dense regions composed of ultra-fine splats, and regions from lower temperature deposits are shown in Table 2.[11]

Table 2 Volume Fractions of Various Coating Deposit Types

Component	Volume Fraction (%)
Voids	19
Dense regions (ultrafine splats)	60
Lower temperature deposits	12

7. Process-Property Relationships

The thermal spray process has a large number of process variables. Here we will present the process-property relationships for a selected few cases. Figure 11 shows the effect of raster scan step height on the prominence of inter-pass boundaries. The porous regions are maximized by retaining more of the unpyrolized precursor that arrives off the centerline of the torch. The results in Fig. 11 are consistent with the notion that small inter-pass raster scan step height is both most efficient in retaining the low-density deposits off the centerline and provides more passes at a give location for the accumulation of low density deposits compared with a larger step height. Making more prominent inter-

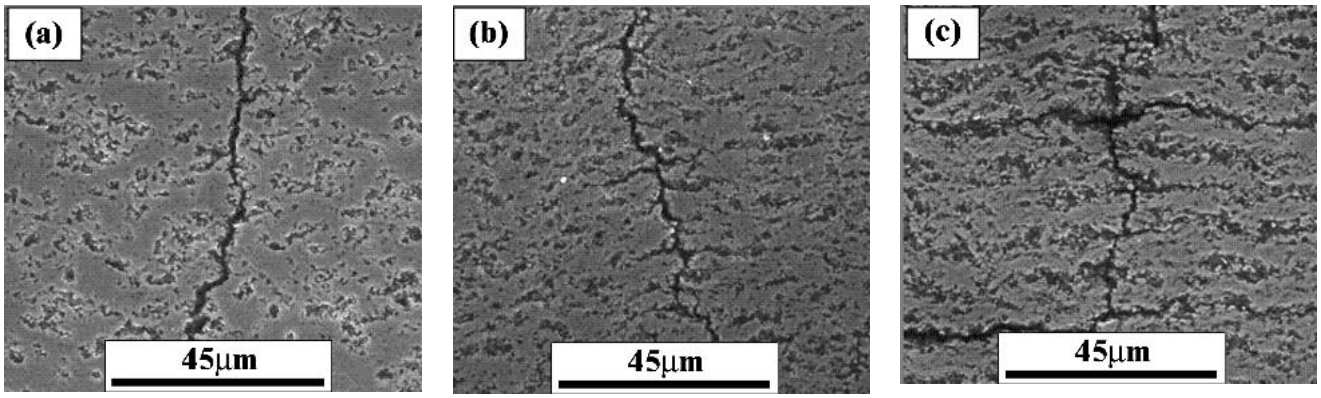

Fig. 11 Effect of plasma torch traverse step size on the appearance of the inter-pass boundaries; the plasma torch transverse step size decreases in the sequence (a-c).

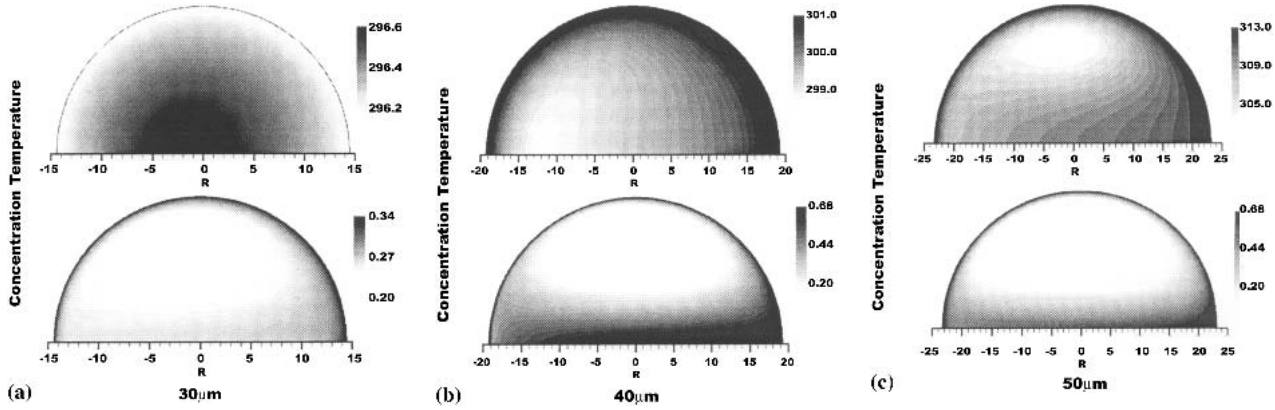

Fig. 12 Calculated droplet temperature and solute concentration for various sized initial droplets[14]

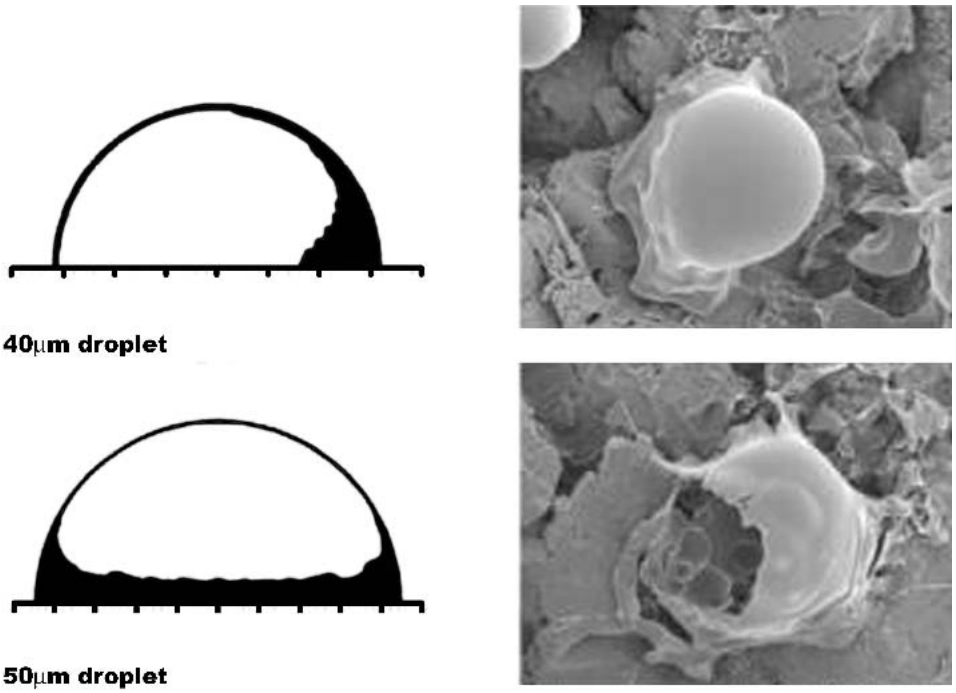

Fig. 13 Calculated regions of high solute concentration compared with hollow shell found in SPPS deposition[14]

pass boundaries is a potential method of making lower conductivity TBCs by the SPPS process.

8. Transport Phenomena

The observed deposits in the SPPS process are almost exclusively of a size that corresponds to spheres smaller than 1-2 μm. From mass balance considerations, a 20 μm droplet when evaporated leads to a ceramic particle about 8 μm in diameter, which is 500 times larger than the volume of the individual observed deposits, indicating that droplet beak-up is a characteristic feature of the SPPS process.

The liquid droplets experience primarily convective heat transfer, which is greatest when the droplet first enters the plasma jet due to the large relative velocity between the droplet and plasma. An axisymmetric, transient droplet transport and heating model has been constructed in which the droplets are allowed to travel in the gas temperature and velocity field of the plasma as constructed in earlier experiments.[14,15] Figure12 shows the temperature field and the associated solute concentration profile caused by evaporation. As is apparent in the figure, solute concentrates rapidly in the surface layer even while including both fluid circulation and solute diffusion in the model.

The precursor used can form both a flexible skin and a solid gel phase, and the simulation results admit the possibility that hollow droplets may form and also that vapor explosion from internal evaporation is one possible mechanism for droplet break-up. Figure 13 shows hollow droplet deposits found in SPPS coatings and the associated solute concentration from modeling.

One additional interesting aspect of the deposition process is worth discussing briefly. The vast bulk of deposits found in SPPS spray experiments involve droplets that are less than 2 μm in diameter. The gas flow field and streamlines must turn and run parallel to the surface upon which it impinges. Sufficiently small particles will turn with the gas flow and not reach the surface, while larger particles having sufficient inertia, will penetrate the boundary layer and will reach the surface. A crude estimate of the likelihood of a particle reaching the surface for the current version of the SPPS process can be made looking at the estimated Stokes numbers defined as $St = \tau_p/\tau_f = V_p D_p/18\mu$, where numbers larger than one would be predictive of the particle hitting the surface. Considering the Stokes numbers of order 1 being the limit, particles with Stokes numbers greater than 1 are those particles with diameters greater than about 10 μm. Work is under way to resolve this fundamental mechanisms issue.

9. Summary

The solution precursor plasma spray process produces coatings with unique microstructures, which have ultrafine splats, nanometer and micron-sized porosity, and through thickness vertical cracks. Careful study of the resulting deposits shows that they consist of 1-2 μm particles that arrive at the coated surface in various stages of conversion from the aqueous precursor to the fully molten ceramic end product. The coating microstructure can be intentionally varied over a wide range by controlling the relative proportions of the different stages of reaction of the precursor. Maximum heating of the precursor leads to dense deposits, while increasing amounts of partially pyrolized precursor leads to greater porosity. The deposition process involves droplet break-up, solute evaporation, and pyrolysis of the

precursor into the ceramic end product. The details of the transport processes of the particles reaching the substrate are not fully understood. Most significantly, the PLPS process results in thermal barrier coatings with attractive properties in terms of thermal conductivity, cost, available maximum thickness, and especially, durability superior to current coatings.

Acknowledgment

The present work was support by the Office of Naval Research under contracts N000014-98-C-0100 and N000014-02-1-0171 with contract managers Dr. Lawrence Kabacoff and Dr. Steven Fishman.

References

1. N. Padture, M. Gell, and E.H. Jordan: "Thermal Barrier Coatings For Gas-Turbine Engine Applications," *Science, 296*(5566), p. 280.
2. A.G. Evans, D.R. Mumm, J.W. Hutchison, G.H. Meier, and F.S. Pettit: "Mechanisms Controlling the Durability of Thermal Barrier Coatings," *Prog. Mater. Sci.* 2001, *46*(5), pp. 505-53.
3. M. Boulos and E. Pfender: "Materials Processing With Thermal Plasmas," *MRS Bull.,* 1996, *21,* p. 65.
4. J. Karthikeyan, C.C. Berndt, S. Reddy, J-Y. Wang, A.H. King, and H. Herman: **"**Nanomaterial Deposits Formed by DC Plasma Spraying of Liquid Feedstocks,**"** *J. Am. Ceram. Soc.,* 1998, *81,* p. 121.
5. S.D. Parkukuttyamma, J. Margolis, H. Liu, C.P. Grey, S. Sampath, H. Herman, and J.B. Parise: "Yttrium Aluminum Garnet (YAG) Films Through a Precursor Plasma Spraying Technique," *J. Am. Ceram. Soc.,* 2001, *84,* p. 1906.
6. E. Bouyer, G. Schiller, M. Muller, and R.H. Henne: "Characterization of SiC and Si_3N_4 Coatings Synthesized by Means of Inductive Thermal Plasma From Disilane Precursors," *Appl. Oganomet. Chem.* 2001, *15,* p. 833.
7. N.P. Padture, K.W. Schlichting, T. Bhatia, A. Ozturk, B. Cetegen, E.H.Jordan, M. Gell, S. Jiang, T.D. Xiao, P.R. Strutt, E. Garcia, P. Miranzo, and M.I. Osendi: "Towards Durable Thermal Barrier Coatings with Novel Microstructres Deposited by Solution-Precursor Plasma Spray," *Acta Mater.,* 2001, *49,* p. 2251.
8. T. Bhatia, A. Ozturk, L. Xie, E. Jordan, B. Cetegen, M. Gell, X. Ma, and N. Padture: "Mechanisms of Ceramic Coating Deposition in Solution-Precursor Plasma Spray," *J. Mater. Res.,* 2002 *17*(9), p. 2363.
9. L. Xie, X. Ma, E.H. Jordan, N.P. Padture, T.D. Xiao, and M. Gell: "Identification of Coating Deposition Mechanisms in the Solution-Precursor Plasma-Spray Process using Model Spray Experiments," *Mater. Sci. Eng. A,* 2003, in press.
10. A. Ozturk and B.M. Cetegen: "Plasma Assisted Deposition of Nanostructured Yttria Stabilized Zirconia Coatings from Liquid Precursors" in Chemical and Physical Processes of Combustion: The 2001 Technical Meeting of Eastern States Section of Combustion Institute, Hilton Head, SC, 2001, pp. 304-07.
11. L. Xie, X. Ma, E.H. Jordan, N.P. Padture, T.D. Xiao, and M. Gell: "Deposition of Thermal Barrier Coatings Using the Solution Precursor Plasma Spray Process," *J. Mater. Sci. Technol.,* 2003, in press.
12. B. Shafiro and M. Kachanov: "Anisotropic Effective Conductivity of Materials With Non-Randomly Oriented Inclusions of Diverse Ellipsoidal Shapes," *J. Appl. Phys.,* 2000, *87*(12), pp. 8561-69.
13. A. Ozturk and B.M. Cetegen: "Nucleation of Zirconia in a Droplet Stream of Liquid Precursor Processed by Flat Premixed Flame," Paper No. F21*,* The Third Joint Technical Meeting of the U. S. Sections of the Combustion Institute, Chicago, IL, March 17-19, 2003.
14. S.Y. Semenov and B.M. Cetegen: "Spectroscopic Temperature Measurements in DC-Arc Plasma Jets Utilized in Thermal Spray Processing Of Materials," *J. Therm. Spray Technol.,* 2001, *10*(2), p. 326.
15. S.Y. Semenov: "Experimental Diagnostics and Modeling of Thermal Spray Deposition Processes of Nano-structured Wear Resistant and Thermal Barrier Coatings," Doctor of Philosophy Thesis, University of Connecticut (2002).